Journal of Water Process Engineering 42 (2021) 102057

Contents lists available at ScienceDirect

Journal of Water Process Engineering

journal homepage: www.elsevier.com/locate/jwpe

Electrocoagulation of a chocolate industry wastewater in a Downflow column electrochemical reactor

V.M. García-Orozco [a], G. Roa-Morales [a,*], Ivonne Linares-Hernández [b], I.J. Serrano-Jimenes [a], M. A. Salgado-Catarino [a], R. Natividad [a,*]

[a] Centro Conjunto de Investigación en Química Sustentable UAEM-UNAM, Universidad Autónoma del Estado de México, Carretera Toluca-Atlacomulco, Km 14.5, Campus San Cayetano, Toluca, MEX, 50200, Mexico

[b] Instituto Interamericano de Tecnología y Ciencias de Agua (IITCA), Universidad Autónoma del Estado de México, Km.14.5, carretera Toluca-Atlacomulco, Toluca, Estado de México, C.P 50200, Mexico

ARTICLE INFO

Keywords:
Hydrogen production
Aluminium electrodes
Food industry
Electrochemical reactors
Electrocoagulators

ABSTRACT

Electrocoagulation is a process that consists in the production of coagulant species by the dissolution of a sacrificial anode. This work presents by the first time the performance of a Downflow Column Electrochemical Reactor (DCER) to conduct an electrocoagulation process to remove organic and inorganic matter from wastewater (6 L) of a chocolate industry. A deep flow battery connected to a solar panel was used to energize the aluminium electrodes. The studied variables were electrical current (*I:* 1.58 A and 3.16 A) and liquid volumetric flowrate (Q_L: 0.032 L/s and 0.060 L/s). The response variables were COD and color removal (%). It was concluded that during the first 5 min, the interaction of both variables exerts the most significant effect on COD removal, while for the rest of the treatment the effect of I is more statistically significant than Q_L. Regarding color, an 80 % was removed during the first 5 min of treatment. It was also concluded that $I = 3.16$ A and $Q_L = 0.06$ L/s were the conditions to reach the maximum COD and color removal, 63 and 97 %, respectively. In addition, the hydrogen production was theoretically estimated to be 0.26 L after 20 min of treatment. A cost analysis was conducted by taking into account the sludge management, electrode consumption, electricity consumption by electrodes and pump. The calculated cost was 4.01 USD/m^3. A second order adsorption model was found to provide an excellent fitting of the experimental COD and color data.

1. Introduction

World population is constantly growing, and this implies an increased consumption of services, medicines, chemical products, clothes, food and commodities. The environmental impact of these industries is undeniable, and the chocolate industry is not the exception. In order to satisfy the worldwide demand, chocolate is produced in large quantities every year [1,2]. The chocolate industry generates different kind of waste like volatile compounds (di and tri terpenes), flavonoids, polyphenols, pyrroles, methylxanthines, aldehydes, phospholipids mixtures, ketones, liquid cocoa, butter triglycerides, aliphatic alcohols, glycolipids, furans, sterols and saturated fats [3,4]. Therefore, the chocolate industry wastewater must be treated before being discharged and to do so, biological treatments have been preferred. This type of treatments, however, are lengthy and require a fine control of operational variables for the microorganisms to survive [5]. This has motivated the assessment of alternative treatments like the electrochemical ones.

Among electrochemical methods, Electrocoagulation (EC) allows to treat water with organic matter and suspended solids. EC combines flotation, coagulation and oxidation or reduction of pollutant compounds [6]. In EC, an anode and a cathode are necessary to carry out the treatment. The anode works as a sacrificial electrode and by *in-situ* electro-dissolution, provides the system with the coagulating agent. This anode can be made of aluminium, copper, magnesium, iron, zinc and stainless steel [7–9] and in contact with the wastewater leads to hydrolysis products (hydroxo-metal species) that are effective in the destabilization of pollutants. Concomitantly, the reduction of water in the cathode produces hydrogen gas bubbles and hydroxide ions. This increases pH in the bulk solution and produces sludge at the water surface and this facilitates its removal.

When Al electrodes are used, the following reactions are expected to

* Corresponding authors.
E-mail addresses: gabyroam@gmail.com (G. Roa-Morales), rnatividadr@uaemex.mx (R. Natividad).

https://doi.org/10.1016/j.jwpe.2021.102057
Received 21 January 2021; Received in revised form 11 March 2021; Accepted 28 March 2021

proceed [10],

Anode,

$$Al_{(s)} \rightarrow Al^{3+}_{(aq)} + 3e^- \quad (1)$$

Cathode,

$$2H_2O_{(l)} + 2e^- \rightarrow H_{2(g)} + 2OH^-_{(aq)} \quad (2)$$

In aqueous medium the following reactions might take place (Eqs. 3–4) [11–13],

$$Al^{3+} + 3(OH)^- \rightarrow Al(OH)_{3(s)} \quad (3)$$

$$nAl(OH)_3 \rightarrow Al_n(OH)_{3n} \quad (4)$$

Different pollutants that have been successfully removed by EC are dyes, suspended solids, heavy metals, fluorides, hardness, arsenic, phosphates and pesticides [14–19]. This process is typically conducted in batch electrochemical cells with continuous stirring. At industrial scale, however, this might lead to mass transfer limitations thus reducing pollutants removal effectiveness. In addition, the electricity consumption sometimes limits the application of EC. This work aimed to assess a rather novel technology in the field of electrochemistry, a Downflow Column Electrochemical Reactor (DCER). This in an ejector type reactor that was originally conceived as gas absorber. Later on, it evolved as three-phase reactor [20]. This is the first work where such a technology is applied to conduct an electrocoagulation process. Aluminium electrodes were used and an effluent from the chocolate industry was treated. Thus, the effectiveness of the process was established. It is also worth pointing out that the electrodes were energized by a deep flow battery connected to a solar panel in order to reduce the cost by electricity consumption.

2. Materials and methods

2.1. Wastewater samples

The wastewater is typically transported from a chocolate industry to a treatment plant. The sampling was conducted right before entering the treatment plant. The wastewater was collected in 20 L plastic containers and kept at 4 °C until treatment. However, the characterization was conducted within 24 h of collection.

2.2. Electrocoagulation treatment

DCER consists of a downward parallel flow column, that is shaped like a cylinder (100 cm of height and 5 cm of diameter) with a capacity of 2 L. The system is depicted in Fig. 1. It can be observed that the liquid phase is fed at the top of the column and recirculated through the whole system during the total treatment time. This technology exploits an orifice at the top of the column to produce a Venturi effect that promotes mass transfer. The breaking vessel is a 5 L stainless steel reservoir with the following dimensions (20×10^{-2} m in diameter and 15.9×10^{-2} m in height). There is a stainless-steel coil heat exchanger placed inside this reservoir. By means of this coil, the temperature is kept constant since the pump transfers thermal energy to the solution. The aluminium electrodes (one pair of plates for the anode and one pair for the cathode) were placed inside the column. Between each pair of aluminium plates there was a 0.5 cm gap and between the anode and cathode the separation distance was 1×10^{-2} m, the aluminium plates dimensions were 92.5×10^{-2} m in length, 0.318×10^{-2} m of thickness and a width of 2.4×10^{-2} m. The total volume occupied by the electrodes was 0.282 L and therefore the total free volume inside the column was 1.682 L. Nevertheless, at all experiments a total volume of 6 L was used and the studied liquid volumetric flowrates were 0.032 and 0.06 L/s. The samples (20×10^{-3} L) were taken at the point indicated in Fig. 1. The energy was supplied by a deep flow battery charged by a solar panel, connected to a charge controller. This arrangement allowed to have a constant electrical current during the whole treatment despite using solar energy. The electrical current supplied was 1.58 and 3.16 A. The initial conductivity of the sample (785.8 μS/cm) was not enough to achieve the aforementioned electrical current values. Thus, sodium sulfate (1 M) was added in order to increase the conductivity up to 1680 μS/cm. The working pH was 6.4 (initial pH of the wastewater sample). At all experiments, the treatment time was 1 h and were carried out by duplicate.

2.3. Methods of analysis

The wastewater sample characterization was carried out according to APHA [21]. In this context, turbidity, pH, color, total and faecal coliforms, chemical oxygen demand (COD), biochemical oxygen demand (BOD_5), electrical conductivity, sulphates, nitrites, nitrates, ammoniacal nitrogen, phosphates, fluorides, chlorides, Fe, Cu, Na, K, Mg, Al and Ca were determined.

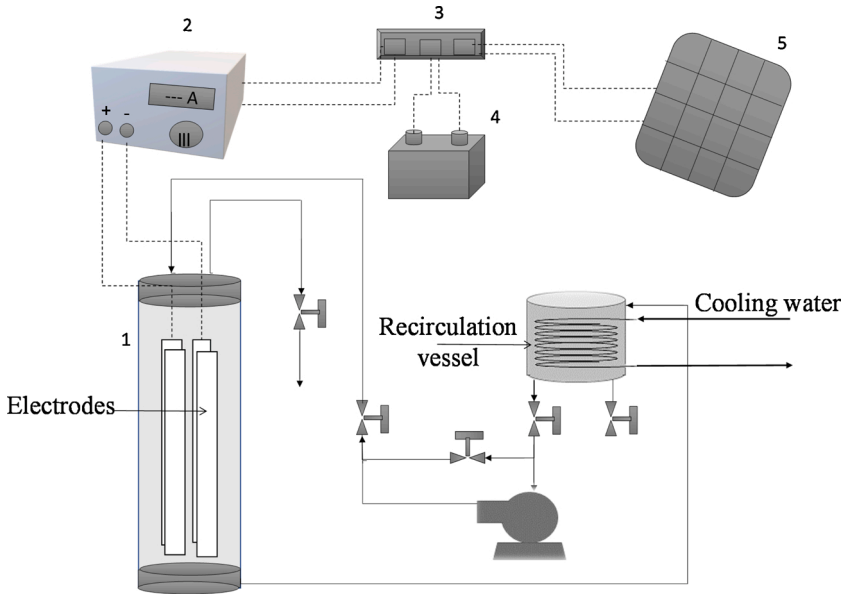

Fig. 1. Experimental set up used for the electrocoagulation treatment. 1) Downflow Column Electrochemical Reactor (DCER), 2) Current control, 3) Solar charge controller, 4) Battery, 5) Solar Panel and 6) Breaking vessel.

For turbidity, a 20 mL sample was analysed in a HF Scientific® Micro100 Laboratory Turbidimeter. The pH was monitored with a pH meter HANNA HI98190 and the electrical conductivity with an ion450 Radiometer.

Regarding color, the samples (10 mL) were not filtered before this analysis. Thus, the reported results correspond to the apparent colour. This parameter was measured in a HACH $DR_{5000.}$ Spectrometer, at 455 nm according to the Pt-Co color method.

For the analysis of fluorides, 0.5 mL of TISAB II solution were added to 5 mL of sample and the concentration of F^- was determined by a selective electrode with a HANNA HI83308 instruments potentiometer.

Nitrites and ammoniacal nitrogen were determined by the HACH method using the reagents TNT 835 and TNT 83, respectively.

The metals concentration (Fe, Cu, Na, K, Mg, Al and Ca) was determined by atomic absorption with a SpectrAA 240 FS spectrophotometer.

The following analyses were performed using Mexican standards: total and faecal coliforms (NMX-AA-42−1987), chemical oxygen demand (COD) (NMX-AA-030/2-SCFI-2011) in a HACH DR_{5000} Spectrometer, biochemical oxygen demand (BOD_5) (NMX-AA-028-SCFI-2001) in a HANNA HI 2400 instrument, phosphates (NMX-AA-029-SCFI-2001) was analysed by a colorimetric method, chlorides (NMX-AA-073-SCFI-2001) was analysed by a colorimetric titrimetric method, nitrates (NMX-AA-079-SCFI-2001) and sulphates (NMX-AA-074-SCFI-2014), by using a lambda 25 UV–vis Perkin Elmer Spectrometer.

The sludge was quantified by determination of settleable solids in raw and treated wastewater in mL/L according to the mexican standard NMX-AA-004-SCFI-2000 [22]. Once the sample was filtered, the sludge was dried for 24 h at 105 °C and then weighed.

2.4. Gas production

In order to determine the volume of produced gas, the shutting-down method was applied. This consists in simultaneously closing down the inlet and the exit valve of the DCER and switching off the pump. By this means the gas dispersion (bubbles) collapses and a gas volume is observed on top of the liquid phase. Since the column was made of transparent glass, this allowed to measure the volume occupied by the produced gas.

The plausible composition of the produced gas was established by considering the stoichiometry of the reactions where the expected gases (H_2, O_2, N_2 and Cl_2) are being produced and also consumed. This analysis and its results are presented in section 3.3.

2.5. Species formation and quantification

In order to establish the conditions (pH interval) at which the Al $(OH)_3$ is predominant given a specific Al(III) concentration and the ionic strength, a speciation diagram was generated via MEDUSA program [23]. The speciation diagram was generated at 3.16 A and at 30 min of treatment.

The ionic strength was calculated by using the ions concentration according to Eq. 5 [24],

$$I_s = (1/2)\sum z_i^2 c_i \tag{5}$$

Here, I_s is ionic strength, c_i is concentration (mol/L), z_i is the ionic charge and the summation was carried out for all ionic species present in the medium ((Fe^{2+}, Cu^{2+}, Na^+, K^+, Mg^{2+}, Al^{3+} and Ca^{2+}).

The amount of material released from the anode to the solution was calculated by Faraday's law (Eq. 6) [25],

$$EC_{Electrode}\left(kg/m^3\right) = I{\cdot}t{\cdot}MA/(n_{e^-}{\cdot}F{\cdot}v * 1000) \tag{6}$$

Where F is the Faraday's constant (96,485 C/mol), I is electrical current (A), t is time (s), v is volume (m^3), n_{e^-} is equal to the number of electrons and MA is Al atomic mass (g/mol).

The Faradaic efficiency was calculated under the best treatment conditions by means of Eq. 7 [26],

$$FE(\%) = OC/TC \tag{7}$$

Where *OC (observed coagulant)* is the experimentally determined mass of coagulant (kg/m^3) and *TC* (Theoretical coagulant) is the amount of coagulant released $EC_{Electrodo}$ (kg/m^3) calculated by Eq. 6.

The resulting ionic strength was 0.042 M and the Al(III) concentration was 3.28 mM. These values were used to generate the speciation diagram with the purpose of ensuring that the flocs ($Al(OH)_3$), responsible for the organic and inorganic matter removal, are being electrogenerated at the treatment pH.

2.6. Cost analysis

According to literature [27–32], the cost of the EC treatment is the sum of the energy cost and electrode wear. In this work, the energy consumption of the pump and the cost generated by the sludge management were added as shown in Eq. 8 [33],

$$Operation\ Cost = aEC_{Electrode\ energy} + bEC_{Pump\ energy} + cEC_{Electrode} + dEC_{sludge} \tag{8}$$

where $EC_{\text{ Electrode}}$ is expressed as kg Al lost/m^3, $EC_{\text{ Sludge}}$ in kg/m^3, $EC_{\text{ Electrode energy}}$ and $EC_{\text{ Pump energy}}$ as kWh/ m^3, a equal to b (0.04 USD/kWh) [34], c (2.008 USD /kg Al lost) and d is the cost of sludge confinement in Mexico (0.035 USD/kg) [33].

To establish the cost of the energy consumed by the pump (1.119 kW) and electrodes during the treatment, Eq. 9 was used [35],

$$EC_{Electrode\ energy}\ or\ EC_{Pump\ energy}\left(kWh/m^3\right) = (I{\cdot}U{\cdot}t_1)/(v * 1000) \tag{9}$$

Where U is voltage in V, t_1 is time (h), I (electrical current in A) and v (volume in m^3). In Mexico, the energy cost is $ 0.956 (MXN currency) per kWh [36], the exchange rate for MXN to USD was considered as 1 USD = 22.68 MXN.

3. Results and discussion

3.1. Physicochemical characterization of industrial wastewater

The physicochemical characteristics of the chocolate industry wastewater before EC treatment are summarized in Table 1. The initial sample pH was 6.4 and was not adjusted at any time. All the experiments were carried out at this initial value. The chocolate industry sample showed a high organic content, COD (1732 mg/L) and BOD_5 (1399.8 mg/L), the biodegradability index (BOD_5/COD) was 0.8, so the wastewater sample was easily biodegradable. In addition, apparent color (1560 Pt-Co Units) and turbidity (512.4 NTU) were ascribed to a high content of colloidal matter, so this type of water is suitable to be treated by EC. The sample also had microbiological matter, faecal and total coliforms (1.4×10^6 and 1.7×10^6 MPN). This is because a fraction of the wastewater comes from the toilets. This also explains the presence of nitrogen in the form of nitrites and nitrates [37]. The inorganic matter was also quantified (711.4 mg/L SO_4^{2-}). This amount is the available for precipitation with the electrogenerated coagulant. The determined phosphates concentration (26.9 mg/L) is low in the context of chocolate industry wastewater. It is worth noticing that the removal of phosphorous and nitrogen is important to reduce excessive growth of algae and the oxygen depletion of the water body at the time of being discharged. Fluorides (0.3 mg/L) and chlorides (169.7 mg/L) were also detected. Chlorides might oxidize at the anode and indirectly promote the oxidation of organic matter by producing chlorine gas or hypochlorite in aqueous solution.

The physicochemical characterization and the determination of anions and cations were of great importance to calculate the ionic strength

Table 1
Physicochemical Characteristics of wastewater before and after EC treatment.

Parameter	Units	Before EC	After EC	Removal (%)
pH	–	6.4	7.4	–
Turbidity	NTU	512.4	37.8	92.6
Color	Pt-Co	1560	48.5	96.9
Total coliforms	MPN/100 mL	1.7×10^6	<200	–
Fecal coliforms	MPN/100 mL	1.4×10^6	<200	–
COD	mg/L	1732	640.5	63
BOD_5	mg/L	1399.8	329.6	76.5
Conductivity	μS/cm	1680	1495	11
Sulfates	SO_4^{2-} mg/L	711.4	519.8	26.9
Nitrites	$N\text{-}NO_2^-$ mg/L	0.9	0.4	55.6
Nitrates	$N\text{-}NO_3^-$ mg/L	1.4	1.1	21.4
Ammoniacal nitrogen	N- NH_3 mg/L	10	18	–
Phosphate	PO_4^{3-} mg/L	26.9	15.9	40.9
Fluoride	F^- mg/L	0.3	0.04	86.7
Chlorides	Cl^- mg/L	169.7	117.2	30.9
Fe	mg/L	1.4	0.6	57.1
Cu	mg/L	0.6	0.5	16.7
Na	mg/L	251.2	185.4	26.2
K	mg/L	10.4	8	23.1
Mg	mg/L	14.65	5.1	65.2
Al	mg/L	1.6	99.5 (14.09[a] at pH = 9)	–
Ca	mg/L	30.3	16.7	44.9

[a] After precipitation.

(0.042 M) and to generate the speciation diagram (figure S1). According to this diagram, at pH = 6.4, $Al(OH)_3$ is produced. This occurs by means of reaction 3, and this resulted in a pH increase.

There are in Mexico two standards that regulate the pollutants concentration in waters to be discharged either in rivers and lakes (NOM-001-SEMARNAT-1996 [38]) or in the municipal sewage (NOM-002--SEMARNAT-1996 [39]). According to these standards, the daily discharge of BOD_5 and Cu should not be higher than 150 and 15 mg/L, respectively. From the contaminants found in the chocolate industry wastewater (Table 1), only these two are regulated.

Table 1 also summarizes the results of the physicochemical characterization of the wastewater after 30 min of treatment under $I = 3.16$ A and $Q_L = 0.06$ L/s. As shown in section 3.2, these were the experimental conditions at which the maximum COD and Color removal were achieved in the shortest time. As can be seen in Table 1, the pH at the end of the treatment increased to 7.4 and this was ascribed to the produced aluminum hydroxides. Organic parameters as COD decreased from 1732 to 640.5 mg/L, achieving a removal efficiency of 63 %. BOD was reduced from 1399.8–329.6 mg/L (76.5 %). Thus, the biodegradability index also decreased to 0.5, which is consistent with less biodegradable matter after applying the EC treatment. Turbidity and color were successfully removed, 92.6 % and 96.9 %, respectively. This can be ascribed to the suspended colloids being eliminated by their adsorption in the flocs. Microbiological parameters were decreased considerably. After EC treatment, faecal and total coliforms <200 MPN /100 mL were detected. Inorganic anions, like sulphates, were removed (26.9 %) probably as aluminium sulfate. According to speciation diagrams the optimum precipitation of sulphates is pH 2–4, so the initial sample pH (6.4) did not favor this mechanism. Phosphates were also diminished (40.9 %). Nevertheless, this removal percentage was not as high as expected and this could be ascribed to two reasons, the first one is related to the soluble chemical form at pH 6.4, as di-hydrogen and hydrogen phosphate ($H_2PO_4^-$ and HPO_4^{2-}). According to the speciation diagram, phosphates can precipitate at pH 12. The second reason of low removal could be associated to a relative low concentration of aluminum hydroxide, that although efficiently removes COD and color, was not enough to act as a chelating agent for phosphates and other anions.

On the other hand, an increase of ammoniacal nitrogen from 10 mg/L to 18 mg/L was observed. This could be associated to the oxidation of organic nitrogen, due to the formation of chlorine gas by the anodic oxidation of chloride ions, according to Eq. 10,

$$2Cl^- \rightarrow Cl_2 + 2e^- \quad (10)$$

ClO^- might be produced by Eq. 11,

$$H_2O + Cl_2 \rightarrow 2ClO^- + 2H^+ \quad (11)$$

These species are also responsible for the disinfection process.

Nitrates were reduced from 1.4 to 1.1 mg/L (21.4 %) and nitrites from 0.9 to 0.4 mg/L (55.4 %). This could be ascribed to the following electrochemical reactions [40],

$$NO_3^- + H_2O + 2e^- \rightarrow NO_2^- + 2OH^- \quad (12)$$

$$NO_3^- + 3H_2O + 5e^- \rightarrow 1/2N_2 + 6OH^- \quad (13)$$

$$NO_3^- + 6H_2O + 8e^- \rightarrow NH_3 + 9OH^- \quad (14)$$

$$NO_2^- + 2H_2O + 3e^- \rightarrow 1/2N_2 + 4OH^- \quad (15)$$

$$NO_2^- + 5H_2O + 6e^- \rightarrow NH_3 + 7OH^- \quad (16)$$

$$NO_2^- + 4H_2O + 4e^- \rightarrow NH_2OH + 5OH^- \quad (17)$$

$$NO_3^- + 2H_2O \rightarrow NH_3 + 2O_2 + OH^- \quad (18)$$

According to these reactions, nitrite ions act as intermediate products and further react with water to generate nitrogen gas, ammonia and hydroxylamine (NH_2OH). Reduction of nitrate to nitrogen gas is the desired process but ammonia is usually formed, and this might be the main reason for the ammoniacal nitrogen to increase after the EC treatment (see Table 1).

Although Mexican Standards (NOM-001-SEMARNAT-1996 and NOM-002-SEMARNAT-1996) [38,39] do not regulate the Al concentration, this was calculated with Faraday's law. The measured concentration in a sample without pH adjustment (to avoid solids precipitation) was 99.5×10^{-3} kg/m^3. The difference between the theoretical (88.35×10^{-3} kg/m^3) and measured Al concentration could be associated to the super faradaic efficiency [41] which was calculated to be 112.6 % by means of Eq. 7.

3.2. Effect of electrical current and volumetric flowrate

Fig. 2 shows there is an important effect of I on both, COD and colour removal. According to Fig. 2, the liquid volumetric flowrate also exerts an important effect on COD removal but not on colour. This effect is more pronounced in the first minutes of treatment and will be further discussed later in this section. The effect of electrical current was expected because enhances anodic dissolution and therefore the amount of Al released into solution. Actually, the results in Fig. 2 suggest this step, the released of the Al into solution, as limiting of the process.

When changing liquid volumetric flowrate what is actually changing is the contact time and the space velocity within the column where the electrodes are placed. In this work, this contact time (τ) refers to the time that the liquid volume where the electrodes are placed (1.68 L) spends in contact with the electrodes and it can also be defined as the time per pass per the electrochemical section. It is worth to remember that in this section the following steps are occurring: *i*) the electrochemical generation of Al^{3+} (reaction 1), *ii*) the transport of such ions to the bulk solution, *iii*) formation of coagulating species (reactions 3–4) and *iv*) bonding of certain pollutants to the coagulating species. It is also worth clarifying that steps *iii* and *iv* might proceed also in the rest of the system, i.e. piping, pump and breaking vessel. Thus, contact time is the available time for step *i* and *ii* to proceed per pass and not per treatment. The

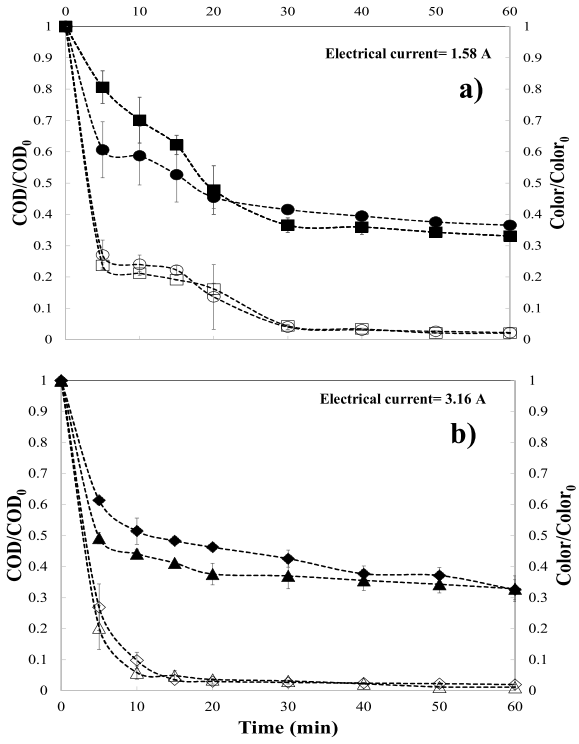

Fig. 2. Effect of electrical current and treatment time on normalized Chemical Oxygen Demand (COD) a) 1.58 A and b) 3.16 A, at Q_L 0.06 L/s and 0.032 L/s for COD (0.06 L/s ■, 0.032 L/s ●, 0.06 L/s ▲ and 0.032 L/s ◆) and Color (0.06 L/s □, 0.032 L/s ○, 0.06 L/s Δ and 0.032 L/s ◊).

latter, treatment time, is the total time that the liquid was recirculated through the whole system until the energy source was off. This treatment time was 1 h for all experiments.

Two liquid volumetric flowrates were tested, 0.032 L/s and 0.06 L/s. The corresponding contact times were 53 and 28 s, respectively. If this time is used in the Faraday Law, the amount of Al^{3+} per pass can be calculated. Table 2 summarizes these values also as a function of applied electrical current.

Also, it can be observed in Table 2 the effect of liquid volumetric flowrate and *I* on the initial COD removal rate. It can be observed that there is not an effect on initial COD removal rate of applied electrical current at low volumetric flowrates. Since the generated Al^{3+} per pass increases when the applied electrical current increases, then the observed increase in initial COD removal rate when the volumetric flowrate and the applied current increase, can be ascribed to an improvement in step *i* and in mass transport, so the other two steps are also enhanced. The mass transport would be enhanced due to the increase in velocity and therefore in turbulence. When only Q_L is increased and *I* is kept at its lowest value, $-r_{COD,o}$ decreases despite the higher turbulence associated to the increase in velocity. This can be ascribed to the lower amount of Al^{3+} generated per pass (see Table 2).

Table 2
Theoretical amount of generated Al^{3+} as a function of contact time and electrical applied current.

Volumetric flowrate	Velocity	Contact time	Electrical current	Theoretical amount of Aluminium	Initial removal rate, $-r_{COD,o}$ (mg/L·min)
(L/s)	(m/s)	(s)	(A)	(mg/pass)	
0.06	0.036	28.03	1.58	4.13	67.2
0.06	0.036	28.03	3.16	8.26	175.9
0.032	0.019	52.56	1.58	7.74	136.4
0.032	0.019	52.56	3.16	15.48	133.8

Fig. 3 shows the effect of both variables, electrical current and liquid volumetric flowrate, on pH profiles. It can be observed that at all experiments, pH increases when treatment time increases. The liquid volumetric flowrate affects the increase on pH only at low electrical currents while its effect is practically negligible at the highest applied electrical current. The observed increase in pH is due to the generation of hydroxide ions in the medium [42].

In order to establish the statistical significance of each studied variable, a two-factor (Q_L and *I*) ANOVA with two replicas was conducted. The response variables were color and COD removal. Table 3 summarizes the results of the aforementioned statistical analysis within a 95 % level of confidence ($P = 0.05$). The relative value of *F* (variances ratio) was the criterion to decide whether or not the effect of a variable was statistically significant. If $F_{cal} > F_{crit}$ then the effect was considered significant [43]. Hence, from the results shown in Table 3, it can be concluded that regarding color the effect of *I* is more significant than Q_L effect. This is truth only after 5 min of treatment. In the first 5 min none of the studied variables appear to be more significant than the other.

Regarding COD removal, the results in Table 3 indicate that the statistical significance of each variable changes with time. Interestingly enough, in the first 5 min of treatment, the factor that exerts the most significant effect is the interaction of both variables, Q_L and *I*. After 5 min, however, the variable with the most significant effect is only *I*. This confirms that what limits the process in the first 5 min of treatment is the concentration of Al^{3+} into solution, which is dictated by steps *i* and *ii*. A higher Q_L not only improves mass transfer by increasing turbulence but also contributes to homogenize the Al^{3+} concentration in a shorter time than at a lower Q_L. After 5 min the factor with the most significant effect is *I*. This suggests a merely chemical step becoming the controlling one after five minutes. This can be either step *iii* or *iv*. Step *iii* might be discarded since pH in the first 15 min only varies between 6.4 and 7 and therefore only $Al(OH)_3$ is expected according to the speciation diagram. Step *iv*, however, not only depends on the concentration of the coagulating species but on the chemical affinity between these species and the ones remained in solution. After 5 min, a change in slope is evident in Fig. 2. This indicates that the compounds with chemical affinity with the coagulant species are being depleted. Therefore, it can be concluded that after 5 min step *iv* becomes the controlling step because the concentration of the species to chemically bound to the coagulant has decreased.

3.3. Cost analysis

In this work, the electrode consumption was 88.35×10^{-3} kg Al lost/m^3, the electrode energy consumption was 2.54 kWh/m^3, the pump

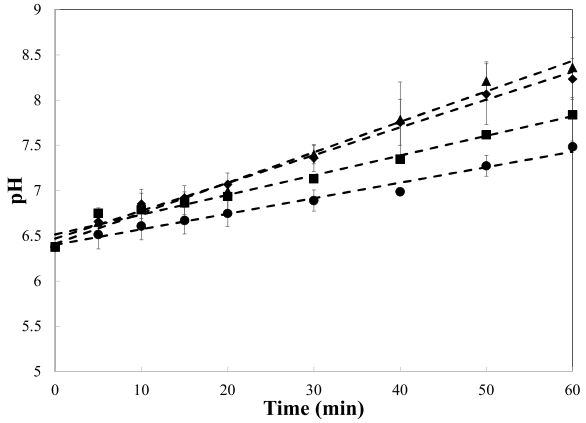

Fig. 3. Effect of electrical current and volumetric flowrate on pH. Electrical current = 1.58 A (0.06 L/s ■ and 0.032 L/s ●) and electrical current = 3.16 A (0.06 L/s ▲ and 0.032 L/s ◆).

Table 3
Statistical significance ($P = 0.05$) of the effect of liquid flowrate and electrical current on Color and COD removal.

$t_{treatment}$ (min)	Factor	F_{cal}		F_{crit}	
		Color	COD	Color	COD
	I	0.19	16.83		
5	Q_L	1.52	1.09		
	I and Q_L interaction	0.15	18.52		
	I	83.17	13.66		
10	Q_L	4.32	0.21	7.7	
	I and Q_L interaction	0.12	4.31		
	I	480.3	14.76		
15	Q_L	1.4	1.22		
	I and Q_L interaction	8.4	6.35		

energy consumption was 93.25 kWh/m^3 and the sludge production was equal to 119.2 × 10^{-3} kg/m^3 (69 mL/L). The cost of this treatment was 4.01 USD/m^3. This cost was calculated taking into account the energy consumed by the pump, the generated sludge and the electrodes wear.

The energy consumption and electrode wear calculated in this work were lower than those reported in other works, albeit to treat other type of wastewater: slaughterhouse wastewater (4.19 ± 0.12 kW h/m^3 and 1.29 ± 0.00 kg/m^3) [44], sugar industry wastewater (42 kW h/m^3 and 0.795 kg/m^3) [45] and dairy industry wastewater (45 kW h and 1.566 kg/m^3) [46]. It is worth pointing out that in these works, COD was removed between 82–96.4%.

The cost of the photovoltaic installation was USD$ 284.68. This was calculated by taking into account the cost of one solar battery of deep cycle CALE of 12 V/110AH (USD $132.78), one Solar Panel IUSA of 375 W (USD$ 138.77) and one Solar charge controller Anself of 20A, 12 V/24 V (USD$13.13). Because the life of solar panels is around 20 years, the investment cost is considered minimum.

3.4. Gas production

During the studied process, the production of H_2, N_2 and Cl_2 gases is expected according to reactions 2, 10, 13 and 15. O_2 generation might be occurring by the following reaction at the anode,

$$2H_2O \rightleftharpoons O_2 + 4H^+ + 4e^- \quad (19)$$

It is worth pointing out that the gas produced was first dispersed in the liquid phase as bubbles and near to the end of treatment, the mixture was accumulated on top of the column. In any case, a displacement of the liquid phase was observed. The displaced liquid volume was accommodated in the breaking vessel (see Fig. 1). The produced volume of gas was quantified by the method described in section 2.5 and it was 0.36 L after 30 min of treatment. Based on this volume and on the stoichiometry of reactions 2 and 19, the theoretical value of produced hydrogen and oxygen was 0.24 L and 0.12, respectively. This would represent the minimum expected H_2 content in the produced gas mixture. However, other authors [47] studied the electrocoagulation of surface water with Al electrodes and determined that the H_2 content was higher than 92.6 % due to reactions 1 and 2 being predominant while reaction 19 was demonstrated to occur but at much lower extent.

Regarding Cl_2, this gas is likely to be consumed via two reactions, Eq. 11 and by reaction with the nitrogen organic matter. Thus, its concentration in the resulting gas mixture can be assumed negligible. Regarding N_2, its theoretical produced volume was calculated by the measured initial and final concentration of NO_3^- and NO_2^-, and by taking into account the stoichiometry of reactions 13 and 15. Based on this, the produced N_2 volume by reactions 15 and 17 after 30 min of treatment would be 1.3 mL and 2.9 mL, respectively. It is worth keeping in mind that these volumes were calculated considering that all the amount of removed nitrites and nitrates were consumed solely by reactions 13 and 15. However, as previously mentioned in section 3.1, these ions are also likely to be consumed in reactions 12, 14, 16 and 18 and therefore the expected produced N_2 is lower than the aforementioned. Thus, as in the case of Cl_2, the total theoretical volume of produced N_2 can be considered negligible in comparison with the theoretical H_2 volume. Based on this analysis the obtained gas is expected to be rich in H_2 (at least 67 % v/v).

We believe that the ability of the system of retaining the hydrogen within the system is an important advantage of this technology for further applications. The hydrogen produced in this way can be continuously taken out of the system and conducted to be used as reagent to other processes like Fischer-Tropsch or CO_2 reduction [48].

3.5. Modelling

One process that takes place at the electrodes surface, specifically at the anode, is the production of Al^{3+} according to reaction (1). The coagulation process then occurs by adsorption of the pollutants onto the flocs that have been formed. Thus, the removal of pollutants by coagulation can be modelled as an adsorption process. In this case a second order adsorption model was tested (Eq. 20),

$$(dq/dt) = k_L(q_e - q)^2 \quad (20)$$

This equation is solved by separating variables and integration considering that $q = 0$ when $t = 0$ and is q_t at any treatment time. The result is given by Eq. 21,

$$(t/q_t) = \left((1)/(k_e q_e^{\,2})\right) + ((1)/(q_e))t \quad (21)$$

where q_t is the concentration of pollutants removed by coagulation at a given treatment time, t, and can be calculated according to Eq. (22),

$$q_t = V(C_0 - C_t)/M \quad (22)$$

where V is the volume of treated wastewater and M is the mass of dissolved electrode, which is a function of the applied current.

By substituting Eq. (22) in (21) and by grouping constants the following equation is obtained,

$$\frac{t}{1-\left(\frac{C_t}{C_0}\right)} = b + m \cdot t \quad (23)$$

where C_t is the chemical oxygen demand (in mg/L) or color at any treatment time t, while C_o is the initial chemical oxygen demand (mg/L) or initial color, $b = C_0((M)/(V))((1)/(k_2 q_e^{\,2}))$ and $m = C_t * ((M)/(V))((1)/(q_e))$, k_2 is the kinetic constant of second order adsorption model. The group of constants b and m, were found by plotting $t/(1 - (C/C_0))$ vs t. The obtained values are summarized in Table 4 for both, color and COD removal.

The excellent fitting of the experimental data by the second order adsorption model is also demonstrated in Fig. 4. Therefore, it can be concluded that the experimental data are well represented by Eq. 24 that is obtained by rearranging Eq. 23,

$$\frac{C_t}{C_o} = 1 - \frac{t}{m + b \cdot t} \quad (24)$$

4. Conclusions

A Downflow Column Electrochemical Reactor was successfully

Table 4
Parameters of second order adsorption model and Determination Coefficients (r^2).

Color removal			COD Removal		
m (min)	b	r^2	m (min)	b	r^2
1.1798	0.9841	0.997	2.7275	1.4776	0.997

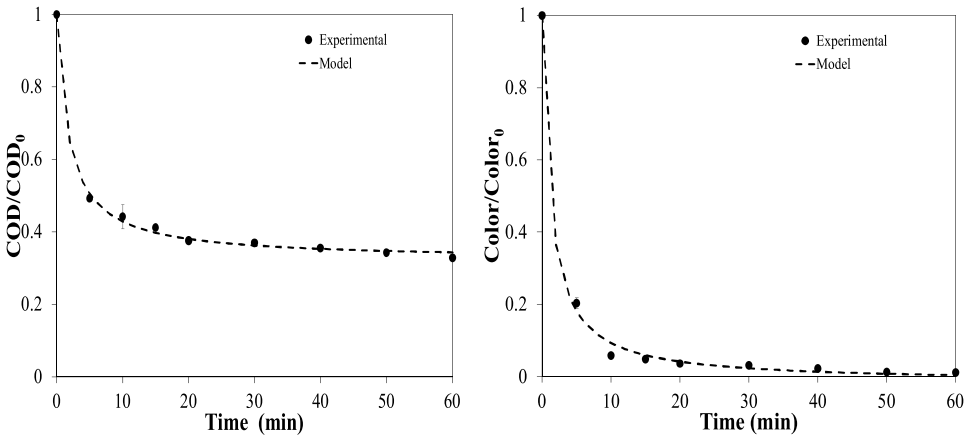

Fig. 4. Comparison of experimental data with predicted data by second order adsorption model: normalized COD and Color as function of time.

assessed by the first time in the electrocoagulation process, using Al electrodes, to remediate wastewater from a chocolate industry. A maximum of COD and color removal, 63 and 97 %, respectively, was reached after 20 min of treatment using an electrical current of 3.16 A and a liquid volumetric flowrate of 0.06 L/s. Approximately 0.26 L of H_2 are produced at this treatment time. It was concluded that the first 5 min of the treatment are critical regarding COD and color removal. In this period of time the interaction of electrical current and liquid volumetric flowrate is the factor with the most significant effect on COD removal. Regarding color removal, it was concluded that there is not an appreciable difference in the effect of any of the studied variables until 10 min where the effect of electrical current became statistically significant.

The cost of this treatment was 4.01 USD/m^3. The treated effluent fulfils the Mexican standard NOM-02-SEMARNAT-1996. The resulting data are well represented by a second order adsorption model

Declaration of Competing Interest

The authors report no declarations of interest.

Acknowledgments

V. García acknowledges CONACYT from Mexico for financial support to conduct postgraduate studies (CVU 626446). The technical support of Citlalit Martínez Soto is also acknowledged.

Appendix A. Supplementary data

Supplementary material related to this article can be found, in the online version, at doi:https://doi.org/10.1016/j.jwpe.2021.102057.

References

[1] N.R. Maddela, D. Kakarla, L.C. García, S. Chakraborty, K. Venkateswarlu, M. Megharaj, Cocoa-laden cadmium threatens human health and cacao economy: a critical view, Sci. Total Environ. (2020) 137645, https://doi.org/10.1016/j.scitotenv.2020.137645.

[2] A. Konstantas, H.K. Jeswani, L. Stamford, A. Azapagic, Environmental impacts of chocolate production and consumption in the UK, Food Res. Int. 106 (2018) 1012–1025, https://doi.org/10.1016/j.foodres.2018.02.042.

[3] I. Magalhães, L.D.F. Vilela, C. Santos, N. Lima, R.F. Schwan, Volatile compounds and protein profiles analyses of fermented cocoa beans and chocolates from different hybrids cultivated in Brazil, Food Res. Int. (2018), https://doi.org/10.1016/j.foodres.2018.04.012.

[4] M. Kindlein, E. Elts, H. Briesen, Phospholipids in chocolate: structural insights and mechanistic explanations of rheological behavior by coarse-grained molecular dynamics simulations, J. Food Eng. (2018), https://doi.org/10.1016/j.jfoodeng.2018.02.014.

[5] M. Esparza-Soto, A. Jacobo-López, M. Lucero-Chávez, C. Fall, Anaerobic treatment of chocolate-processing industry wastewater at different organic loading rates and temperatures, Water Sci. Technol. 79 (2019) 2251–2259, https://doi.org/10.2166/wst.2019.225.

[6] D.T. Moussa, M.H. El-Naas, M. Nasser, M.J. Al-Marri, A comprehensive review of electrocoagulation for water treatment: potentials and challenges, J. Environ. Manage. 186 (2017) 24–41, https://doi.org/10.1016/j.jenvman.2016.10.032.

[7] C. Hu, J. Sun, S. Wang, R. Liu, H. Liu, J. Qu, Enhanced efficiency in HA removal by electrocoagulation through optimizing flocs properties: role of current density and pH, Sep. Purif. Technol. 175 (2017) 248–254, https://doi.org/10.1016/j.seppur.2016.11.036.

[8] A.K. Prajapati, P.K. Chaudhari, D. Pal, A. Chandrakar, R. Choudhary, Electrocoagulation treatment of rice grain based distillery effluent using copper electrode, J Water Process Eng 11 (2016) 1–7, https://doi.org/10.1016/j.jwpe.2016.03.008.

[9] A. Tanner, R. Devlin, M.S. Kowalski, X. Zhang, V. Wei, J.A. Oleszkiewicz, Electrocoagulation of raw wastewater using aluminum, iron, and magnesium electrodes, J. Hazard. Mater. (2018), https://doi.org/10.1016/j.jhazmat.2018.10.017.

[10] P. Durango-Usuga, F. Guzmán-Duque, R. Mosteo, M.V. Vazquez, G. Peñuela, R. A. Torres-Palma, Experimental design approach applied to the elimination of crystal violet in water by electrocoagulation with Fe or Al electrodes, J. Hazard. Mater. 179 (2010) 120–126, https://doi.org/10.1016/j.jhazmat.2010.02.067.

[11] M. Kobya, R.D.C. Soltani, P.I. Omwene, A. Khataee, A review on decontamination of arsenic-contained water by electrocoagulation: reactor configurations and operating cost along with removal mechanisms, Environ Technol Innov 17 (2020), https://doi.org/10.1016/j.eti.2019.100519.

[12] Y. Tian, W. He, D. Liang, W. Yang, B.E. Logan, N. Ren, Effective phosphate removal for advanced water treatment using low energy, migration electric–field assisted electrocoagulation, Water Res. 138 (2018) 129–136, https://doi.org/10.1016/j.watres.2018.03.037.

[13] M. Elazzouzi, A. El Kasmi, K. Haboubi, M.S. Elyoubi, A novel electrocoagulation process using insulated edges of Al electrodes for enhancement of urban wastewater treatment: techno-economic study, Process Saf. Environ. Prot. 116 (2018) 506–515, https://doi.org/10.1016/j.psep.2018.03.006.

[14] A. Dura, C.B. Breslin, Electrocoagulation using aluminium anodes activated with Mg, in and Zn alloying elements, J. Hazard. Mater. 366 (2019) 39–45, https://doi.org/10.1016/j.jhazmat.2018.11.094.

[15] N.S. Graça, A.M. Ribeiro, A.E. Rodrigues, Modeling the electrocoagulation process for the treatment of contaminated water, Chem. Eng. Sci. 197 (2019) 379–385, https://doi.org/10.1016/j.ces.2018.12.038.

[16] K.S. Hashim, N. Jasim, A. Shaw, D. Phipps, P. Kot, A.W. Alattabi, et al., Electrocoagulation as a green technology for phosphate removal from river water, Sep. Purif. Technol. 210 (2019) 135–144, https://doi.org/10.1016/j.seppur.2018.07.056.

[17] B.M.B. Ensano, L. Borea, V. Naddeo, V. Belgiorno, M.D.G. de Luna, M. Balakrishnan, et al., Applicability of the electrocoagulation process in treating real municipal wastewater containing pharmaceutical active compounds, J. Hazard. Mater. (2018), https://doi.org/10.1016/j.jhazmat.2018.07.093.

[18] C. An, G. Huang, Y. Yao, S. Zhao, Emerging usage of electrocoagulation technology for oil removal from wastewater: a review, Sci. Total Environ. 579 (2017) 537–556, https://doi.org/10.1016/j.scitotenv.2016.11.062.

[19] D. Franco, J. Lee, S. Arbelaez, N. Cohen, J.Y. Kim, Removal of phosphate from surface and wastewater via electrocoagulation, Ecol. Eng. 108 (2017) 589–596, https://doi.org/10.1016/j.ecoleng.2017.07.031.

[20] R.P. Fishwick, R. Natividad, R. Kulkarni, P.A. McGuire, J. Wood, J. M. Winterbottom, et al., Selective hydrogenation reactions: a comparative study of monolith CDC, stirred tank and trickle bed reactors, Catal. Today 128 (2007) 108–114, https://doi.org/10.1016/j.cattod.2007.06.030.

[21] APHA/AWWA/WEF, Standard methods for the examination of water and wastewater, Stand Methods 541 (2012).

[22] Nmx-aa-004-scfi-2000. análisis de agua - determinación de sólidos sedimentables e.n. aguas naturales, Residuales Y Residuales TRATADAS - MÉTODO DE PRUEBA (CANCELA A La NMX-AA-004-1977), 2000.

[23] I. Puigdomenech, Hydrochemical Equilibrium Constants Database (MEDUSA), Royal Institute of Technology, Stockholm, Sweden, 1997.

[24] Y. Zhang, C. Zhu, F. Liu, Y. Yuan, H. Wu, A. Li, Effects of ionic strength on removal of toxic pollutants from aqueous media with multifarious adsorbents: a review, Sci. Total Environ. 646 (2019) 265–279, https://doi.org/10.1016/j.scitotenv.2018.07.279.
[25] Q. Feng, K. Zhang, X. Liu, W. Guan, X. Chen, L. Song, et al., An improved kinetic model for dephosphorization of laundry wastewater by electrocoagulation, J Water Process Eng 39 (2021), 101750, https://doi.org/10.1016/j.jwpe.2020.101750.
[26] M. Ingelsson, N. Yasri, E.P.L. Roberts, Electrode passivation, faradaic efficiency, and performance enhancement strategies in electrocoagulation—a review, Water Res. 187 (2020), 116433, https://doi.org/10.1016/j.watres.2020.116433.
[27] S. Bener, Ö Bulca, B. Palas, G. Tekin, S. Atalay, G. Ersöz, Electrocoagulation process for the treatment of real textile wastewater : effect of operative conditions on the organic carbon removal and kinetic study, Process Saf. Environ. Prot. 129 (2019) 47–54, https://doi.org/10.1016/j.psep.2019.06.010.
[28] S.U. Khan, D.T. Islam, I.H. Farooqi, S. Ayub, F. Basheer, Hexavalent chromium removal in an electrocoagulation column reactor: process optimization using CCD, adsorption kinetics and pH modulated sludge formation, Process Saf. Environ. Prot. 122 (2019) 118–130, https://doi.org/10.1016/j.psep.2018.11.024.
[29] V. Ya, N. Martin, K.H. Choo, Y.H. Chou, S.J. Lee, N.C. Le, et al., High-pressure electrocoagulation system with periodic air replenishment for efficient dye wastewater treatment: reaction dynamics and cost evaluation, J. Clean. Prod. 213 (2019) 1127–1134, https://doi.org/10.1016/j.jclepro.2018.12.249.
[30] V.F. Mena, A. Betancor-Abreu, S. González, S. Delgado, R.M. Souto, J.J. Santana, Fluoride removal from natural volcanic underground water by an electrocoagulation process: parametric and cost evaluations, J. Environ. Manage. 246 (2019) 472–483, https://doi.org/10.1016/j.jenvman.2019.05.147.
[31] F.Y. AlJaberi, Operating cost analysis of a concentric aluminum tubes electrodes electrocoagulation reactor, Heliyon 5 (2019), e02307, https://doi.org/10.1016/j.heliyon.2019.e02307.
[32] F. Hussin, F. Abnisa, G. Issabayeva, M.K. Aroua, Removal of lead by solar-photovoltaic electrocoagulation using novel perforated zinc electrode, J. Clean. Prod. 147 (2017) 206–216, https://doi.org/10.1016/j.jclepro.2017.01.096.
[33] L.F. Castañeda, O. Coreño, J.L. Nava, G. Carreño, Removal of fluoride and hydrated silica from underground water by electrocoagulation in a flow channel reactor, Chemosphere 244 (2020), 125417, https://doi.org/10.1016/j.chemosphere.2019.125417.
[34] CFE (Comisión Federal De Electricidad). Consulta Tu Tarifa, 2019 n.d. https://app.cfe.mx/aplicaciones/ccfe/tarifas/tarifas/Tarifas_casa.asp?Tarifa=DACTAR1&anio=2018 (accessed May 19, 2020).
[35] V.M. Garcia Orozco, C.E. Barrera Diaz, G. Roa Morales, I. Linares Hernandez, A comparative electrochemical-ozone treatment for removal of phenolphthalein, J. Chem. 2016 (2016), https://doi.org/10.1155/2016/8105128.
[36] Comisión Federal De Electricidad. Consulta Tu Tarifa, 2019 (accessed May 19, 2020), https://app.cfe.mx/aplicaciones/ccfe/tarifas/tarifas/Tarifas_casa.asp?Tarifa=DACTAR1&anio=2018.
[37] C.-W. Hu, Y.-J. Chang, C.-C. Yen, J.-L. Chen, R.B. Muthukumaran, M.-R. Chao, 15N-labelled nitrite/nitrate tracer analysis by LC-MS/MS: urinary and fecal excretion of nitrite/nitrate following oral administration to mice, Free Radic. Biol. Med. (2019), https://doi.org/10.1016/j.freeradbiomed.2019.08.005.
[38] SEMARNAT. Norma Oficial Mexicana NOM-001-SEMARNAT-1996, Que ESTABLECE Los Límites MÁXIMOS Permisibles De Contaminantes En Las Descargas De Aguas Residuales E.N. Aguas Y. Bienes Nacionales, 1996 (accessed June 22, 2020), http://www.conagua.gob.mx/CONAGUA07/Publicaciones/Publicaciones/SGAA-15-13.pdf.
[39] SEMARNAT. Norma Oficial Mexicana NOM-002-SEMARNAT-1996, Que ESTABLECE Los Límites MÁXIMOS Permisibles De Contaminantes En Las Descargas De Aguas Residuales a Los Sistemas De Alcantarillado Urbano O. Municipal, 1996 (accessed June 23, 2020), http://www.conagua.gob.mx/CONAGUA07/Publicaciones/Publicaciones/SGAA-15-13.pdf.
[40] W.T. Mook, M.H. Chakrabarti, M.K. Aroua, G.M.A. Khan, B.S. Ali, M.S. Islam, et al., Removal of total ammonia nitrogen (TAN), nitrate and total organic carbon (TOC) from aquaculture wastewater using electrochemical technology: a review, Desalination 285 (2012) 1–13, https://doi.org/10.1016/j.desal.2011.09.029.
[41] M. Mechelhoff, G.H. Kelsall, N.J.D. Graham, Super-faradaic charge yields for aluminium dissolution in neutral aqueous solutions, Chem. Eng. Sci. 95 (2013) 353–359, https://doi.org/10.1016/j.ces.2013.03.016.
[42] A. Dura, C.B. Breslin, The removal of phosphates using electrocoagulation with Al−Mg anodes, J Electroanal Chem 846 (2019), 113161, https://doi.org/10.1016/j.jelechem.2019.05.043.
[43] J.M.J.C. Miller, Statistics and chemometrics for analytical chemistry, Pearson education (2018).
[44] M. Asselin, P. Drogui, H. Benmoussa, J.F. Blais, Effectiveness of electrocoagulation process in removing organic compounds from slaughterhouse wastewater using monopolar and bipolar electrolytic cells, Chemosphere 72 (2008) 1727–1733, https://doi.org/10.1016/j.chemosphere.2008.04.067.
[45] O.P. Sahu, P.K. Chaudhari, Electrochemical treatment of sugar industry wastewater: COD and color removal, J Electroanal Chem 739 (2015) 122–129, https://doi.org/10.1016/j.jelechem.2014.11.037.
[46] H.C. Lopes Geraldino, J.I. Simionato, De Souza Freitas, K. Thábata Formicoli, J. C. Garcia, O. De Carvalho Júnior, C. Januario Correr, Eficiência e custo operacional de um sistema de eletrofloculação aplicado ao tratamento de efluente da indústria de laticínio, Acta. Sci. Technol. 37 (2015) 401–408, https://doi.org/10.4025/actascitechnol.v37i3.26452.
[47] A. Bailón-Martínez, T. Pavón-Silva, J.G. Ibanez, G. Roa-Morales, Simultaneous electrocoagulation of dam water and production of hydrogen, World Rev. Sci. Technol. Sustain. Dev 13 (2017) 238–255, https://doi.org/10.1504/WRSTSD.2017.087141.
[48] A.C. Vosloo, Fischer–tropsch: a futuristic view, Fuel Process Technol (2001) 149–155, https://doi.org/10.1016/S0378-3820(01)00143-6.